Measurement of $e^+e^- \to \pi^0\pi^0\psi(3686)$ at $\sqrt{s}$ from 4.009 to 4.600 GeV and observation of a neutral charmoniumlike structure

M. Ablikim,[1] M. N. Achasov,[9,e] S. Ahmed,[14] M. Albrecht,[4] A. Amoroso,[50a,50c] F. F. An,[1] Q. An,[47,a] J. Z. Bai,[1] O. Bakina,[24] R. Baldini Ferroli,[20a] Y. Ban,[32] D. W. Bennett,[19] J. V. Bennett,[5] N. Berger,[23] M. Bertani,[20a] D. Bettoni,[21a] J. M. Bian,[45] F. Bianchi,[50a,50c] E. Boger,[24,c] I. Boyko,[24] R. A. Briere,[5] H. Cai,[52] X. Cai,[1,a] O. Cakir,[42a] A. Calcaterra,[20a] G. F. Cao,[1] S. A. Cetin,[42b] J. Chai,[50c] J. F. Chang,[1,a] G. Chelkov,[24,c,d] G. Chen,[1] H. S. Chen,[1] J. C. Chen,[1] M. L. Chen,[1,a] S. J. Chen,[30] X. R. Chen,[27] Y. B. Chen,[1,a] X. K. Chu,[32] G. Cibinetto,[21a] H. L. Dai,[1,a] J. P. Dai,[35,j] A. Dbeyssi,[14] D. Dedovich,[24] Z. Y. Deng,[1] A. Denig,[23] I. Denysenko,[24] M. Destefanis,[50a,50c] F. De Mori,[50a,50c] Y. Ding,[28] C. Dong,[31] J. Dong,[1,a] L. Y. Dong,[1] M. Y. Dong,[1,a] O. Dorjkhaidav,[22] Z. L. Dou,[30] S. X. Du,[54] P. F. Duan,[1] J. Fang,[1,a] S. S. Fang,[1] X. Fang,[47,a] Y. Fang,[1] R. Farinelli,[21a,21b] L. Fava,[50b,50c] S. Fegan,[23] F. Feldbauer,[23] G. Felici,[20a] C. Q. Feng,[47,a] E. Fioravanti,[21a] M. Fritsch,[14,23] C. D. Fu,[1] Q. Gao,[1] X. L. Gao,[47,a] Y. Gao,[41] Y. G. Gao,[6] Z. Gao,[47,a] I. Garzia,[21a] K. Goetzen,[10] L. Gong,[31] W. X. Gong,[1,a] W. Gradl,[23] M. Greco,[50a,50c] M. H. Gu,[1,a] S. Gu,[15] Y. T. Gu,[12] A. Q. Guo,[1] L. B. Guo,[29] R. P. Guo,[1] Y. P. Guo,[23] Z. Haddadi,[26] A. Hafner,[23] S. Han,[52] X. Q. Hao,[15] F. A. Harris,[44] K. L. He,[1] X. Q. He,[46] F. H. Heinsius,[4] T. Held,[4] Y. K. Heng,[1,a] T. Holtmann,[4] Z. L. Hou,[1] C. Hu,[29] H. M. Hu,[1] T. Hu,[1,a] Y. Hu,[1] G. S. Huang,[47,a] J. S. Huang,[15] X. T. Huang,[34] X. Z. Huang,[30] Z. L. Huang,[28] T. Hussain,[49] W. Ikegami Andersson,[51] Q. Ji,[1] Q. P. Ji,[15] X. B. Ji,[1] X. L. Ji,[1,a] X. S. Jiang,[1,a] X. Y. Jiang,[31] J. B. Jiao,[34] Z. Jiao,[17] D. P. Jin,[1,a] S. Jin,[1] T. Johansson,[51] A. Julin,[45] N. Kalantar-Nayestanaki,[26] X. L. Kang,[1] X. S. Kang,[31] M. Kavatsyuk,[26] B. C. Ke,[5] T. Khan,[47,a] P. Kiese,[23] R. Kliemt,[10] B. Kloss,[23] L. Koch,[25] O. B. Kolcu,[42b,h] B. Kopf,[4] M. Kornicer,[44] M. Kuemmel,[4] M. Kuhlmann,[4] A. Kupsc,[51] W. Kühn,[25] J. S. Lange,[25] M. Lara,[19] P. Larin,[14] L. Lavezzi,[50c,1] H. Leithoff,[23] C. Leng,[50c] C. Li,[51] Cheng Li,[47,a] D. M. Li,[54] F. Li,[1,a] F. Y. Li,[32] G. Li,[1] H. B. Li,[1] H. J. Li,[1] J. C. Li,[1] Jin Li,[33] K. Li,[13] K. Li,[34] Lei Li,[3] P. L. Li,[47,a] P. R. Li,[7,43] Q. Y. Li,[34] T. Li,[34] W. D. Li,[1] W. G. Li,[1] X. L. Li,[34] X. N. Li,[1,a] X. Q. Li,[31] Z. B. Li,[40] H. Liang,[47,a] Y. F. Liang,[37] Y. T. Liang,[25] G. R. Liao,[11] D. X. Lin,[14] B. Liu,[35,j] B. J. Liu,[1] C. X. Liu,[1] D. Liu,[47,a] F. H. Liu,[36] Fang Liu,[1] Feng Liu,[6] H. B. Liu,[12] H. H. Liu,[1] H. H. Liu,[16] H. M. Liu,[1] J. B. Liu,[47,a] J. P. Liu,[52] J. Y. Liu,[1] K. Liu,[41] K. Y. Liu,[28] Ke Liu,[6] L. D. Liu,[32] P. L. Liu,[1,a] Q. Liu,[43] S. B. Liu,[47,a] X. Liu,[27] Y. B. Liu,[31] Y. Y. Liu,[31] Z. A. Liu,[1,a] Zhiqing Liu,[23] Y. F. Long,[32] X. C. Lou,[1,a,g] H. J. Lu,[17] J. G. Lu,[1,a] Y. Lu,[1] Y. P. Lu,[1,a] C. L. Luo,[29] M. X. Luo,[53] T. Luo,[44] X. L. Luo,[1,a] X. R. Lyu,[43] F. C. Ma,[28] H. L. Ma,[1] L. L. Ma,[34] M. M. Ma,[1] Q. M. Ma,[1] T. Ma,[1] X. N. Ma,[31] X. Y. Ma,[1,a] Y. M. Ma,[34] F. E. Maas,[14] M. Maggiora,[50a,50c] Q. A. Malik,[49] Y. J. Mao,[32] Z. P. Mao,[1] S. Marcello,[50a,50c] J. G. Messchendorp,[26] G. Mezzadri,[21b] J. Min,[1,a] T. J. Min,[1] R. E. Mitchell,[19] X. H. Mo,[1,a] Y. J. Mo,[6] C. Morales Morales,[14] G. Morello,[20a] N. Yu. Muchnoi,[9,e] H. Muramatsu,[45] P. Musiol,[4] A. Mustafa,[4] Y. Nefedov,[24] F. Nerling,[10] I. B. Nikolaev,[9,e] Z. Ning,[1,a] S. Nisar,[8] S. L. Niu,[1,a] X. Y. Niu,[1] S. L. Olsen,[33] Q. Ouyang,[1,a] S. Pacetti,[20b] Y. Pan,[47,a] P. Patteri,[20a] M. Pelizaeus,[4] J. Pellegrino,[50a,50c] H. P. Peng,[47,a] K. Peters,[10,i] J. Pettersson,[51] J. L. Ping,[29] R. G. Ping,[1] R. Poling,[45] V. Prasad,[39,47] H. R. Qi,[2] M. Qi,[30] S. Qian,[1,a] C. F. Qiao,[43] J. J. Qin,[43] N. Qin,[52] X. S. Qin,[1] Z. H. Qin,[1,a] J. F. Qiu,[1] K. H. Rashid,[49] C. F. Redmer,[23] M. Richter,[4] M. Ripka,[23] G. Rong,[1] Ch. Rosner,[14] X. D. Ruan,[12] A. Sarantsev,[24,f] M. Savrié,[21b] C. Schnier,[4] K. Schoenning,[51] W. Shan,[32] M. Shao,[47,a] C. P. Shen,[2] P. X. Shen,[31] X. Y. Shen,[1] H. Y. Sheng,[1] J. J. Song,[34] X. Y. Song,[1] S. Sosio,[50a,50c] C. Sowa,[4] S. Spataro,[50a,50c] G. X. Sun,[1] J. F. Sun,[15] S. S. Sun,[1] X. H. Sun,[1] Y. J. Sun,[47,a] Y. K. Sun,[47,a] Y. Z. Sun,[1] Z. J. Sun,[1,a] Z. T. Sun,[19] C. J. Tang,[37] G. Y. Tang,[1] X. Tang,[1] I. Tapan,[42c] M. Tiemens,[26] B. T. Tsednee,[22] I. Uman,[42d] G. S. Varner,[44] B. Wang,[1] B. L. Wang,[43] D. Wang,[32] D. Y. Wang,[32] Dan Wang,[43] K. Wang,[1,a] L. L. Wang,[1] L. S. Wang,[1] M. Wang,[34] P. Wang,[1] P. L. Wang,[1] W. P. Wang,[47,a] X. F. Wang,[41] Y. D. Wang,[14] Y. F. Wang,[1,a] Y. Q. Wang,[23] Z. Wang,[1,a] Z. G. Wang,[1,a] Z. H. Wang,[47,a] Z. Y. Wang,[1] Z. Y. Wang,[1] T. Weber,[23] D. H. Wei,[11] P. Weidenkaff,[23] S. P. Wen,[1] U. Wiedner,[4] M. Wolke,[51] L. H. Wu,[1] L. J. Wu,[1] Z. Wu,[1,a] L. Xia,[47,a] Y. Xia,[18] D. Xiao,[1] H. Xiao,[48] Y. J. Xiao,[1] Z. J. Xiao,[29] Y. G. Xie,[1,a] Y. H. Xie,[6] X. A. Xiong,[1] Q. L. Xiu,[1,a] G. F. Xu,[1] J. J. Xu,[1] L. Xu,[1] Q. J. Xu,[13] Q. N. Xu,[43] X. P. Xu,[38] L. Yan,[50a,50c] W. B. Yan,[47,a] W. C. Yan,[47,a] Y. H. Yan,[18] H. J. Yang,[35,j] H. X. Yang,[1] L. Yang,[52] Y. H. Yang,[30] Y. X. Yang,[11] M. Ye,[1,a] M. H. Ye,[7] J. H. Yin,[1] Z. Y. You,[40] B. X. Yu,[1,a] C. X. Yu,[31] J. S. Yu,[27] C. Z. Yuan,[1] Y. Yuan,[1] A. Yuncu,[42b,b] A. A. Zafar,[49] Y. Zeng,[18] Z. Zeng,[47,a] B. X. Zhang,[1] B. Y. Zhang,[1,a] C. C. Zhang,[1] D. H. Zhang,[1] H. H. Zhang,[40] H. Y. Zhang,[1,a] J. Zhang,[1] J. L. Zhang,[1] J. Q. Zhang,[1] J. W. Zhang,[1,a] J. Y. Zhang,[1] J. Z. Zhang,[1] K. Zhang,[1] L. Zhang,[41] S. Q. Zhang,[31] X. Y. Zhang,[34] Y. Zhang,[1] Y. Zhang,[1] Y. H. Zhang,[1,a] Y. T. Zhang,[47,a] Yu Zhang,[43] Z. H. Zhang,[6] Z. P. Zhang,[47] Z. Y. Zhang,[52] G. Zhao,[1] J. W. Zhao,[1,a] J. Y. Zhao,[1] J. Z. Zhao,[1,a] Lei Zhao,[47,a] Ling Zhao,[1] M. G. Zhao,[31] Q. Zhao,[1] S. J. Zhao,[54] T. C. Zhao,[1] Y. B. Zhao,[1,a] Z. G. Zhao,[47,a] A. Zhemchugov,[24,c] B. Zheng,[48] J. P. Zheng,[1,a] W. J. Zheng,[34] Y. H. Zheng,[43] B. Zhong,[29] L. Zhou,[1,a] X. Zhou,[52] X. K. Zhou,[47,a] X. R. Zhou,[47,a] X. Y. Zhou,[1] Y. X. Zhou,[12,a] K. Zhu,[1] K. J. Zhu,[1,a] S. Zhu,[1] S. H. Zhu,[46] X. L. Zhu,[41] Y. C. Zhu,[47,a] Y. S. Zhu,[1] Z. A. Zhu,[1] J. Zhuang,[1,a] L. Zotti,[50a,50c] B. S. Zou,[1] and J. H. Zou[1]

(BESIII Collaboration)

[1]*Institute of High Energy Physics, Beijing 100049, People's Republic of China*
[2]*Beihang University, Beijing 100191, People's Republic of China*
[3]*Beijing Institute of Petrochemical Technology, Beijing 102617, People's Republic of China*
[4]*Bochum Ruhr-University, D-44780 Bochum, Germany*
[5]*Carnegie Mellon University, Pittsburgh, Pennsylvania 15213, USA*
[6]*Central China Normal University, Wuhan 430079, People's Republic of China*
[7]*China Center of Advanced Science and Technology, Beijing 100190, People's Republic of China*
[8]*COMSATS Institute of Information Technology,*
Lahore, Defence Road, Off Raiwind Road, 54000 Lahore, Pakistan
[9]*G.I. Budker Institute of Nuclear Physics SB RAS (BINP), Novosibirsk 630090, Russia*
[10]*GSI Helmholtzcentre for Heavy Ion Research GmbH, D-64291 Darmstadt, Germany*
[11]*Guangxi Normal University, Guilin 541004, People's Republic of China*
[12]*Guangxi University, Nanning 530004, People's Republic of China*
[13]*Hangzhou Normal University, Hangzhou 310036, People's Republic of China*
[14]*Helmholtz Institute Mainz, Johann-Joachim-Becher-Weg 45, D-55099 Mainz, Germany*
[15]*Henan Normal University, Xinxiang 453007, People's Republic of China*
[16]*Henan University of Science and Technology, Luoyang 471003, People's Republic of China*
[17]*Huangshan College, Huangshan 245000, People's Republic of China*
[18]*Hunan University, Changsha 410082, People's Republic of China*
[19]*Indiana University, Bloomington, Indiana 47405, USA*
[20a]*INFN Laboratori Nazionali di Frascati, I-00044 Frascati, Italy*
[20b]*INFN and University of Perugia, I-06100 Perugia, Italy*
[21a]*INFN Sezione di Ferrara, I-44122 Ferrara, Italy*
[21b]*University of Ferrara, I-44122 Ferrara, Italy*
[22]*Institute of Physics and Technology, Peace Ave. 54B, Ulaanbaatar 13330, Mongolia*
[23]*Johannes Gutenberg University of Mainz, Johann-Joachim-Becher-Weg 45, D-55099 Mainz, Germany*
[24]*Joint Institute for Nuclear Research, 141980 Dubna, Moscow region, Russia*
[25]*Justus-Liebig-Universitaet Giessen, II. Physikalisches Institut,*
Heinrich-Buff-Ring 16, D-35392 Giessen, Germany
[26]*KVI-CART, University of Groningen, NL-9747 AA Groningen, Netherlands*
[27]*Lanzhou University, Lanzhou 730000, People's Republic of China*
[28]*Liaoning University, Shenyang 110036, People's Republic of China*
[29]*Nanjing Normal University, Nanjing 210023, People's Republic of China*
[30]*Nanjing University, Nanjing 210093, People's Republic of China*
[31]*Nankai University, Tianjin 300071, People's Republic of China*
[32]*Peking University, Beijing 100871, People's Republic of China*
[33]*Seoul National University, Seoul 151-747, Korea*
[34]*Shandong University, Jinan 250100, People's Republic of China*
[35]*Shanghai Jiao Tong University, Shanghai 200240, People's Republic of China*
[36]*Shanxi University, Taiyuan 030006, People's Republic of China*
[37]*Sichuan University, Chengdu 610064, People's Republic of China*
[38]*Soochow University, Suzhou 215006, People's Republic of China*
[39]*State Key Laboratory of Particle Detection and Electronics,*
Beijing 100049, Hefei 230026, People's Republic of China
[40]*Sun Yat-Sen University, Guangzhou 510275, People's Republic of China*
[41]*Tsinghua University, Beijing 100084, People's Republic of China*
[42a]*Ankara University, 06100 Tandogan, Ankara, Turkey*
[42b]*Istanbul Bilgi University, 34060 Eyup, Istanbul, Turkey*
[42c]*Uludag University, 16059 Bursa, Turkey*
[42d]*Near East University, Nicosia, North Cyprus, Mersin 10, Turkey*
[43]*University of Chinese Academy of Sciences, Beijing 100049, People's Republic of China*
[44]*University of Hawaii, Honolulu, Hawaii 96822, USA*
[45]*University of Minnesota, Minneapolis, Minnesota 55455, USA*
[46]*University of Science and Technology Liaoning, Anshan 114051, People's Republic of China*
[47]*University of Science and Technology of China, Hefei 230026, People's Republic of China*
[48]*University of South China, Hengyang 421001, People's Republic of China*
[49]*University of the Punjab, Lahore 54590, Pakistan*
[50a]*University of Turin, I-10125 Turin, Italy*
[50b]*University of Eastern Piedmont, I-15121 Alessandria, Italy*
[50c]*INFN, I-10125 Turin, Italy*

[51]Uppsala University, Box 516, SE-75120 Uppsala, Sweden
[52]Wuhan University, Wuhan 430072, People's Republic of China
[53]Zhejiang University, Hangzhou 310027, People's Republic of China
[54]Zhengzhou University, Zhengzhou 450001, People's Republic of China

(Received 30 October 2017; published 7 March 2018)

Using e^+e^- collision data collected with the BESIII detector at the BEPCII collider corresponding to an integrated luminosity of 5.2 fb^{-1} at center-of-mass energies ($\sqrt{s}$) from 4.009 to 4.600 GeV, the process $e^+e^- \to \pi^0\pi^0\psi(3686)$ is studied for the first time. The corresponding Born cross sections are measured and found to be half of those of the reaction $e^+e^- \to \pi^+\pi^-\psi(3686)$. This is consistent with the expectation from isospin symmetry. Furthermore, the Dalitz plots for $\pi^0\pi^0\psi(3686)$ are accordant with those of $\pi^+\pi^-\psi(3686)$ at all energy points, and a neutral analog to the structure in $\pi^\pm\psi(3686)$ around 4040 MeV/c^2 first observed at $\sqrt{s} = 4.416$ GeV is observed in the isospin neutral mode at the same energy.

DOI: 10.1103/PhysRevD.97.052001

I. INTRODUCTION

The vector charmoniumlike state $Y(4360)$ was observed and subsequently confirmed in $e^+e^- \to (\gamma_{\rm ISR})\pi^+\pi^-\psi(3686)$ by *BABAR*, Belle, and BESIII [1–3], where $\gamma_{\rm ISR}$ refers to an initial state radiation (ISR) photon. However, the nature of the $Y(4360)$ remains mysterious [4], as is the case for other states of the Y family, e.g. the $Y(4260)$ observed in $e^+e^- \to (\gamma_{ISR})\pi^+\pi^- J/\psi$ [5–8]. Many theoretical interpretations have been proposed to explain the underlying structure of the Y family of states [9–11]. It is therefore compelling to study the $Y(4360)$ in its $\pi^0\pi^0$ transition to $\psi(3686)$ and to examine isospin symmetry.

In recent years, a new pattern of charmoniumlike states, the $Z_c^\pm$'s, has been observed in the systems of a charged pion and a low-mass charmonium state [3,7,12–14], as well as in charmed mesons pairs [15–17]. The observation of $Z_c^\pm$ particles and of similar states in the bottomonium system [18] indicates the discovery of a new class of hadrons [19]. More recently, neutral charmoniumlike states, which are referred to as Z_c^0's, have been reported in analogous systems [20–23]. These are regarded as the neutral isospin partners of the $Z_c^\pm$'s. A charmoniumlike structure observed in $e^+e^- \to \pi^+\pi^-\psi(3686)$ by BESIII [3] was also reported in Belle's latest updated result [2]. By analogy, it is interesting to search for its neutral isospin partner in $e^+e^- \to \pi^0\pi^0\psi(3686)$.

In this paper, we present a study of the process $e^+e^- \to \pi^0\pi^0\,\psi(3686)$ at c.m. energies ($\sqrt{s}$) from 4.009 to 4.600 GeV. The corresponding Born cross sections are measured for the first time. A new neutral structure is observed in the $\pi^0\psi(3686)$ invariant-mass spectra around 4040 MeV/c^2. The data samples used in this analysis were collected with the BESIII detector at 16 different c.m. energies with a total integrated luminosity of 5.2 fb^{-1} [24]. The c.m. energies have been measured with dimuon events for each energy point [25].

II. BESIII EXPERIMENT AND THE DATA SETS

BEPCII is a double-ring e^+e^- collider running at c.m. energies between 2.0 and 4.6 GeV and reaches a peak luminosity of 1.0×10^{33} cm^{-2} s^{-1} at a c.m. energy of 3770 MeV. The cylindrical BESIII detector has an effective geometrical acceptance of 93% of 4π and divides into a barrel section and two end caps. It contains a small cell, helium-based (60% He, 40% C_3H_8) main drift chamber (MDC), which provides momentum measurement of a charged particle with a resolution of 0.5% at a momentum

[a]Also at State Key Laboratory of Particle Detection and Electronics, Beijing 100049, Hefei 230026, People's Republic of China.
[b]Also at Bogazici University, 34342 Istanbul, Turkey.
[c]Also at the Moscow Institute of Physics and Technology, Moscow 141700, Russia.
[d]Also at the Functional Electronics Laboratory, Tomsk State University, Tomsk 634050, Russia.
[e]Also at the Novosibirsk State University, Novosibirsk 630090, Russia.
[f]Also at the NRC "Kurchatov Institute", PNPI, 188300 Gatchina, Russia.
[g]Also at University of Texas at Dallas, Richardson, TX 75083, USA.
[h]Also at Istanbul Arel University, 34295 Istanbul, Turkey.
[i]Also at Goethe University Frankfurt, 60323 Frankfurt am Main, Germany.
[j]Also at Key Laboratory for Particle Physics, Astrophysics and Cosmology, Ministry of Education; Shanghai Key Laboratory for Particle Physics and Cosmology; Institute of Nuclear and Particle Physics, Shanghai 200240, People's Republic of China.

of 1 GeV/c in a magnetic field of 1 T. The energy loss measurement (dE/dx) provided by the MDC has a resolution better than 6%. A time-of-flight system consisting of 5-cm-thick plastic scintillators can measure the flight time of charged particles with a time resolution of 80 ps in the barrel and 110 ps in the end caps. An electromagnetic calorimeter (EMC) consisting of 6240 CsI (Tl) in a cylindrical structure and two end caps is used to measure the energies of photons and electrons. The energy resolution of the EMC is 2.5% in the barrel and 5.0% in the end caps for a photon/electron of 1 GeV energy. The position resolution of the EMC is 6 mm in the barrel and 9 mm in the end caps. A muon system (MUC) consisting of 1000 m^2 of resistive plate chambers is used to identify muons and provides a spatial resolution better than 2 cm. The detailed description of the BESIII detector can be found in Ref. [26].

The GEANT4-based [27] Monte Carlo (MC) simulation software package BOOST [28] is used to generate MC samples. Simulated MC samples for the signal process $e^+e^- \to \pi^0\pi^0\psi(3686)$ with $\psi(3686) \to \pi^+\pi^- J/\psi$, $J/\psi \to \ell^+\ell^-$, and $\ell = e/\mu$ [referred to as $e^+e^- \to \pi^0\pi^0\psi(3686)$ throughout this paper] and the background process $e^+e^- \to \pi^+\pi^-\psi(3686)$ with $\psi(3686) \to \pi^0\pi^0 J/\psi$ and $J/\psi \to \ell^+\ell^-$ [referred to as $e^+e^- \to \pi^+\pi^-\psi(3686)$ throughout this paper] are generated at each c.m. energy. The e^+e^- collision is simulated with the KKMC [29] generator incorporating the beam energy spread and ISR, where the cross section line shapes of $e^+e^- \to \pi^0\pi^0\psi(3686)$ and $e^+e^- \to \pi^+\pi^-\psi(3686)$ are assumed to be the same and are taken from the latest results from Belle [2]. The processes $e^+e^- \to \pi^{0/+}\pi^{0/-}\psi(3686)$ and $\psi(3686) \to \pi^{+/0}\pi^{-/0}J/\psi$ are simulated with the JPIPI model [30] of EVTGEN [31]. As in Refs. [3,14], the inclusive MC samples at $\sqrt{s} = 4.258$ and 4.358 GeV are used to study the potential backgrounds.

III. EVENT SELECTION

The signal candidates are required to have four charged tracks with zero net charge and at least four photon candidates. The selection criteria for good charged tracks and photons; the separation between pions, electrons, and muons; as well as the hit number required in the muon system for the $\mu^+\mu^-$ pair are the same as those in Ref. [3].

A four-constraint (4C) kinematic fit imposing energy-momentum conservation under the hypothesis $e^+e^- \to \gamma\gamma\gamma\gamma\pi^+\pi^-\ell^+\ell^-$ is performed, and $\chi^2_{4C} < 120$ is required. For the events with more than four photons, the combination of $\gamma\gamma\gamma\gamma\pi^+\pi^-\ell^+\ell^-$ with the least χ^2_{4C} is retained. The pairing of photons into the two π^0 is chosen by minimizing $(M(\gamma_1\gamma_2) - M(\pi^0))^2 + (M(\gamma_3\gamma_4) - M(\pi^0))^2$. The J/ψ and π^0 candidates are selected by requiring $3.05 < M(\ell^+\ell^-) < 3.15$ GeV/c^2 and $|M(\gamma_i\gamma_j) - M(\pi^0)| < 20$ MeV/c^2, where $M(\pi^0)$ is the π^0 mass according to the Particle Data Group (PDG) [32]. A seven-constraint (7C) kinematic fit with additional constraints on the two π^0 and J/ψ masses [32] is imposed to suppress the non-$\pi^0\pi^0\pi^+\pi^- J/\psi$ backgrounds and improve the mass resolution.

IV. EXTRACTION OF THE BORN CROSS SECTION

Figure 1 shows the scatter plots of the $\pi^+\pi^-$ recoil mass $M_{\rm recoil}(\pi^+\pi^-) \equiv \sqrt{(E_{cm} - E(\pi^+\pi^-))^2/c^4 - |\overrightarrow{p_{cm}} - \overrightarrow{p(\pi^+\pi^-)}|^2/c^2}$ versus $M(\pi^+\pi^- J/\psi)$ and the $M(\pi^+\pi^- J/\psi)$ spectra for the data samples at $\sqrt{s} = 4.226$, 4.258, 4.358, 4.416, and 4.600 GeV, which have relatively large statistics. Here, $\overrightarrow{p_{cm}}$ and $\overrightarrow{p(\pi^+\pi^-)}$ refer to the three momentum of c.m. and reconstructed $\pi^+\pi^-$ system respectively, E_{cm} and $E(\pi^+\pi^-)$ are the energy of c.m. and $\pi^+\pi^-$ system. Vertical and horizontal bands at the $\psi(3686)$ mass position are observed clearly in the scatter plots, corresponding to the processes $e^+e^- \to \pi^0\pi^0\,\psi(3686)$ and $e^+e^- \to \pi^+\pi^-\psi(3686)$, respectively. The narrow peaks in the $M(\pi^+\pi^- J/\psi)$ spectra indicate the signal process $e^+e^- \to \pi^0\pi^0\psi(3686)$, while the relative broad bumps with position depending upon the c.m. energy are from $e^+e^- \to \pi^+\pi^-\psi(3686)$.

The inclusive and exclusive MC samples, as well as the data in the J/ψ sideband region (selected by applying a six-constraint kinematic fit without the J/ψ mass constraint instead of the 7C kinematic fit), are used to investigate the backgrounds. The dominant background is $e^+e^- \to \pi^+\pi^-\psi(3686)$ with $\psi(3686) \to \pi^0\pi^0 J/\psi$, which has the same final states as the signal. An unbinned maximum likelihood fit is performed to the $M(\pi^+\pi^- J/\psi)$ spectra to determine the signal yields. In the fit, the probability density functions (PDFs) of $e^+e^- \to \pi^0\pi^0\psi(3686)$ and $e^+e^- \to \pi^+\pi^-\psi(3686)$ are described with the MC simulated shapes convolved with a Gaussian function, where the parameters of the Gaussian function are determined in the fit, in order to account for the resolution difference and potential mass shift between the data and MC simulation. The other backgrounds are described with a linear function. The fits curves are shown in Fig. 1, and the signal yields ($N^{\rm obs}$) from the fit are shown in Table I.

The Born cross section is calculated from

$$\sigma^{\rm B} = \frac{N^{\rm obs}}{\mathcal{L}_{\rm int}(1+\delta^{\rm r})(1+\delta^{\rm v})\mathcal{B}\epsilon}, \qquad (1)$$

where $\mathcal{L}_{\rm int}$ is the integrated luminosity; $N^{\rm obs}$ is the signal yield from the fit; $(1+\delta^{\rm r})$ is the ISR correction factor which is obtained by using a QED calculation [33] and incorporating the input line shape of the cross section, which is taken to be the same as that of $e^+e^- \to \pi^+\pi^-\psi(3686)$ from the Belle experiment [2]; $(1+\delta^{\rm v})$ is the vacuum polarization factor taken from a QED calculation with an accuracy of 0.5% [34]; $\mathcal{B} = 3.89\%$ is the product of the branching fractions in the decay chain, taken from the PDG [32]; and ϵ is the detection efficiency. The

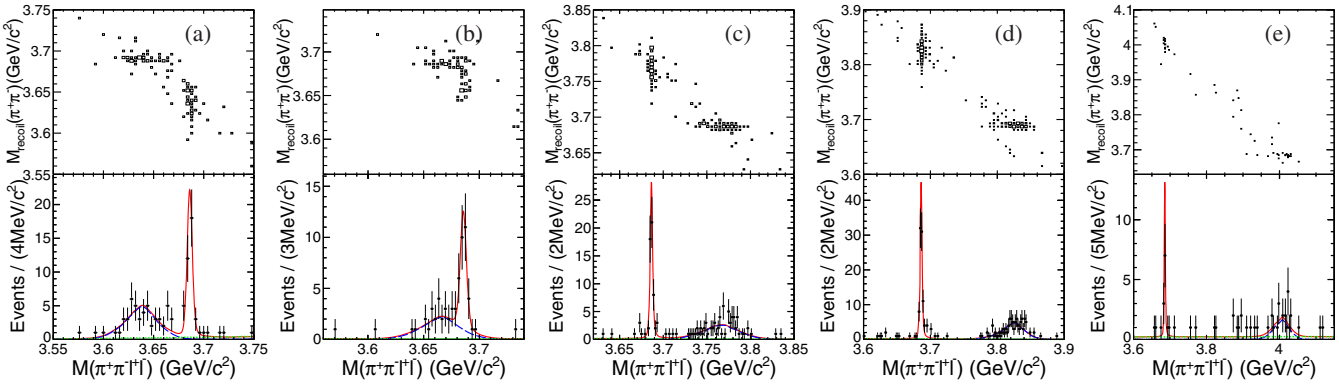

FIG. 1. Scatter plots of $M_{\rm recoil}(\pi^+\pi^-)$ versus $M(\pi^+\pi^-l^+l^-)$ (top) and the $M(\pi^+\pi^-l^+l^-)$ spectra (bottom). Dots with error bars are data; the solid curves show the results of the best fits; the dashed (blue) curves show the results for the background $e^+e^- \to \pi^+\pi^-\psi(3686)$; the short dashed (green) curves show the results for the other backgrounds. The different columns show data at $\sqrt{s}$ = (a) 4.226, (b) 4.258, (c) 4.358, (d) 4.416, and (e) 4.600 GeV, respectively.

numbers used in the Born cross section calculation and the cross sections are summarized in Table I. The comparison of the Born cross section of $e^+e^- \to \pi^0\pi^0\psi(3686)$ to that of $e^+e^- \to \pi^+\pi^-\psi(3686)$ for the data samples with large luminosities is shown in Fig. 2. An alternative fit to the $M_{\rm recoil}(\pi^+\pi^-)$ spectra, which have a narrow peak for $e^+e^- \to \pi^+\pi^-\psi(3686)$ and a broad bump depending on the c.m. energy for $e^+e^- \to \pi^0\pi^0\psi(3686)$, is performed. In the fit, the PDF is described by a similar strategy with the $M(\pi^+\pi^- J/\psi)$ spectra. The Born cross sections of $e^+e^- \to \pi^+\pi^-\psi(3686)$ are also calculated with the corresponding event yields and are consistent with the results in Ref. [3]. The resulting Born cross sections of $e^+e^- \to \pi^0\pi^0\psi(3686)$ are consistent with the nominal values.

For the data samples with small luminosities, only a small number of events survives. The events within $3.676 < M_{\rm recoil}(\pi^+\pi^-) < 3.696$ GeV/c^2 are removed to suppress backgrounds from $e^+e^- \to \pi^+\pi^-\psi(3686)$. Upper limits at the 90% C.L. on the Born cross sections are determined by using a frequentist method with a profile likelihood treatment of systematic uncertainties [35]. The number of signal events ($N^{\rm obs}$) is counted in the region $3.671 < M(\pi^+\pi^- J/\psi) < 3.701$ GeV/c^2, while the number of background events ($N^{\rm bkg}$) is evaluated in the region $3.630 < M(\pi^+\pi^- J/\psi) < 3.660$ GeV/c^2 or $3.712 < M(\pi^+\pi^- J/\psi) < 3.742$ GeV/c^2. In the calculation, the observed events are assumed to have a Poisson distribution, and the event selection efficiencies are assumed to follow a Gaussian distribution. The upper limits are shown are shown in Table I.

The cross section ratios, $R_{\pi^+\pi^-\psi(3686)} = \frac{\sigma(e^+e^-\to\pi^0\pi^0\psi(3686))}{\sigma(e^+e^-\to\pi^+\pi^-\psi(3686))}$, are calculated for data samples with

TABLE I. Summary of Born cross sections for the process $e^+e^- \to \pi^0\pi^0\psi(3686)$ and the ratios $R_{\pi^+\pi^-\psi(3686)}$. $N^{\rm obs}$ is the number of signal events by fitting $\psi(3686)$ for large luminosities and by counting in the signal region of $\psi(3686)$ for small luminosities without subtracting background.

$\sqrt{s}$ (GeV)	$\mathcal{L}_{\rm int}$ (pb^{-1})	$N^{\rm obs}$	$N^{\rm bkg}$	$(1+\delta^{\rm r})$	$(1+\delta^{\rm v})$	ε (%)	$\sigma^{\rm B}$ (pb)	$R_{\pi^+\pi^-\psi(3686)}$
4.008	482.0	0	0	0.70	1.056	10.8	<1.2	···
4.085	52.6	0	0	0.75	1.056	10.2	<11.4	···
4.189	43.1	1	0	0.76	1.056	10.3	<25.0	···
4.208	54.6	2	1	0.76	1.057	10.4	<26.1	···
4.217	54.1	4	0	0.79	1.057	10.5	<44.0	···
4.226	1091.7	37.9 ± 6.6	···	0.76	1.056	10.3	$10.8 \pm 1.9 \pm 0.9$	$0.51 \pm 0.09 \pm 0.03$
4.242	55.6	1	0	0.75	1.053	10.2	<19.9	···
4.258	825.7	29.0 ± 6.4	···	0.76	1.054	10.7	$10.5 \pm 2.3 \pm 0.8$	$0.50 \pm 0.12 \pm 0.03$
4.308	44.9	2	1	0.75	1.053	11.3	<32.5	···
4.358	539.8	60.8 ± 7.8	···	0.79	1.051	11.8	$29.6 \pm 3.8 \pm 2.3$	$0.48 \pm 0.06 \pm 0.03$
4.387	55.2	5	2	0.87	1.051	11.0	<38.8	···
4.416	1073.6	95.5 ± 10.1	···	0.95	1.053	11.7	$19.5 \pm 2.0 \pm 1.6$	$0.46 \pm 0.05 \pm 0.03$
4.467	109.94	3	0	1.08	1.055	9.1	<14.3	···
4.527	109.98	2	0	1.30	1.055	8.2	<11.1	···
4.575	47.7	1	1	1.20	1.055	8.2	<15.5	···
4.600	566.9	10.7 ± 3.5	···	1.09	1.055	9.1	$4.7 \pm 1.6 \pm 0.5$	$0.32 \pm 0.11 \pm 0.03$

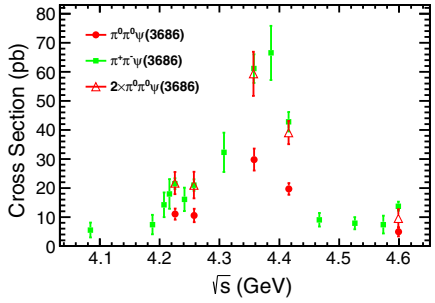

FIG. 2. Born cross section of $e^+e^- \to \pi^0\pi^0\psi(3686)$ at $\sqrt{s} = 4.226$, 4.258, 4.358, 4.416, 4.600 GeV, respectively. The dots (red) are the results obtained in this analysis, and the squares (blue) are the Born cross section of $e^+e^- \to \pi^+\pi^-\psi(3686)$ from Ref. [3]. We multiplied the $e^+e^- \to \pi^0\pi^0\psi(3686)$ cross section by 2 in order to compare it with cross section of $e^+e^- \to \pi^+\pi^-\psi(3686)$. The triangles (red) are twice our results.

large luminosities and are shown in Table I, where $\sigma(e^+e^- \to \pi^+\pi^-\psi(3686))$ are taken from Ref. [3]. A set of common systematic uncertainties among the two processes, including those on luminosity, tracking efficiencies, and the requirements on the lepton tracks, cancel in the calculation. The weighted average of the ratios at $\sqrt{s} =$ 4.226, 4.258, 4.358, 4.416 GeV is $0.48 \pm 0.04 \pm 0.02$. Within uncertainties, the resulting $R_{\pi^+\pi^-\psi(3686)}$ is consistent with the value of 0.5 expected from isospin symmetry, shown in Fig. 2.

V. SYSTEMATIC UNCERTAINTIES ON BORN CROSS SECTION MEASUREMENT

The following sources of systematic uncertainty are considered in the cross section measurements. The uncertainty on the efficiency for charged tracks (photons) is 1% per track (photon) [36,37]. The uncertainty on the hit number requirement in the muon counter is 4.2%, obtained by studying a sample of $e^+e^- \to \pi^+\pi^- J/\psi$ events. The uncertainty related with the kinematic fit is estimated by the same method as in Ref. [38] and is in the range 0.3% to 1.2% depending on the c.m. energy. The uncertainties of the π^0 and J/ψ invariant-mass requirements are evaluated by tuning the corresponding MC distributions according to data and are in the ranges 0.2% to 0.5% and 0.1% to 0.3%, respectively, depending on the c.m. energy. The uncertainties related to the fit procedure are investigated by varying the fit range, replacing the linear function for the background by a second-order polynomial function for background, and varying the width of the Gaussian function for the signal and are in the range 1.6% to 7.3% depending on the c.m. energy. For the data samples with large luminosity, the detection efficiencies are estimated by the MC samples reweighted according to the Dalitz plots distributions of $M^2(\pi^0\psi(3686))$ versus $M^2(\pi^0\pi^0)$ found in the data. The corresponding uncertainty is estimated by varying the weighting factors according to the statistical uncertainty in each bin. For the data samples with low luminosity, the detection efficiencies are estimated with the JPIPI model MC samples. The corresponding systematic uncertainties are estimated with the data samples with large luminosity by comparing the efficiencies derived from the JPIPI model MC sample with the nominal model. The uncertainty associated with the ISR correction factor is studied by replacing the input cross section line shape with the latest results from *BABAR* [1] in the KKMC generator and is in the range 0.3% to 2.4% depending on the c.m. energy. The uncertainty of the vacuum polarization factor is 0.5% from a QCD approach [34].

The uncertainty of the integrated luminosity is 1%, as determined with large-angle Bhabha events [24]. The uncertainties of the branching fractions of the intermediate states are taken from the PDG [32]. A summary of all considered systematic uncertainties is shown in Table II. Assuming all sources of systematic errors are independent, the total uncertainties are the quadratic sums of the individual values, ranging from 7.8% to 10.8%, depending on the c.m. energy.

TABLE II. Summery of systematic uncertainties (%) in the measurement of Born cross section $e^+e^- \to \pi^0\pi^0\psi(3686)$.

Source/$\sqrt{s}$ GeV	4.008	4.085	4.189	4.208	4.217	4.226	4.242	4.258	4.308	4.358	4.387	4.416	4.467	4.527	4.575	4.600
Tracking	4.0	4.0	4.0	4.0	4.0	4.0	4.0	4.0	4.0	4.0	4.0	4.0	4.0	4.0	4.0	4.0
Photon	4.0	4.0	4.0	4.0	4.0	4.0	4.0	4.0	4.0	4.0	4.0	4.0	4.0	4.0	4.0	4.0
MUC cut	4.2	4.2	4.2	4.2	4.2	4.2	4.2	4.2	4.2	4.2	4.2	4.2	4.2	4.2	4.2	4.2
Kinematic fit	0.4	0.5	0.6	0.8	0.9	1.2	0.9	0.8	0.7	0.9	0.5	1.1	2.1	0.8	1.0	0.3
Mass window π^0	0.4	0.5	0.4	0.3	0.3	0.3	0.4	0.4	0.3	0.2	0.4	0.3	0.3	0.3	0.3	0.3
Mass window J/ψ	0.1	0.1	0.1	0.3	0.1	0.1	0.1	0.1	0.1	0.3	0.2	0.2	0.3	0.4	0.3	0.3
Fitting	...	...	...	...	...	4.3	...	3.4	...	2.4	...	1.6	...	...	...	7.3
MC Model	3.3	3.3	3.3	3.3	3.3	1.6	3.3	1.7	3.3	1.4	3.3	1.6	3.3	3.3	3.3	3.3
ISR factor	0.4	0.7	1.8	0.6	0.6	0.5	0.6	1.0	0.3	0.7	2.0	2.1	2.3	2.4	1.1	0.3
Vacuum polarization	0.5	0.5	0.5	0.5	0.5	0.5	0.5	0.5	0.5	0.5	0.5	0.5	0.5	0.5	0.5	0.5
Luminosity	1.0	1.0	1.0	1.0	1.0	1.0	1.0	1.0	1.0	1.0	1.0	1.0	1.0	1.0	1.0	1.0
Branching fraction	1.1	1.1	1.1	1.1	1.1	1.1	1.1	1.1	1.1	1.1	1.1	1.1	1.1	1.1	1.1	1.1
Sum	7.8	8.0	8.2	8.0	8.0	8.7	8.0	8.3	8.0	7.8	8.2	8.0	8.3	8.3	8.1	10.8

VI. STUDY OF INTERMEDIATE STATES

Possible intermediate states in $e^+e^- \to \pi^0\pi^0\psi(3686)$ are investigated using the data samples at $\sqrt{s} = 4.226$, 4.258, 4.358, and 4.416 GeV. The $\psi(3686)$ signal is extracted by selecting the events in the mass range $3.676 < M(\pi^+\pi^-\ell^+\ell^-) < 3.696$ GeV/c^2. The Dalitz plots $M^2(\pi^0\pi^0)$ versus $M^2(\pi^0\psi(3686))$ as well as the corresponding one-dimensional distributions are shown in Fig. 3. Good agreement of these distributions with those observed in the charged mode in Ref. [3] is found, which confirms the variations of the kinematic behavior at different energy points and demonstrates isospin conservation. A structure with a mass around 4040 MeV/c^2 in the $M(\pi^0\psi(3686))$ spectrum is observed in the data sample at $\sqrt{s} = 4.416$ GeV, while two bumps around 3900 and 4040 MeV/c^2 are evident in the data sample at $\sqrt{s} = 4.258$ GeV. It is worth noting that for the data sample at $\sqrt{s} = 4.226$ GeV this structure is not observed in the $M(\pi^0\psi(3686))$ distribution. The behavior observed is similar to that in the charged mode [3]. The dominant background is $e^+e^- \to \pi^+\pi^-\psi(3686)$ as shown in Fig. 1. The other backgrounds are found to be negligible from the study of the sideband region.

An unbinned maximum likelihood fit is performed to the Dalitz plot of $M^2(\pi_1^0\psi(3686))$ versus $M^2(\pi_2^0\psi(3686))$ [denoted as x and y in Eq. (2), respectively] to determine the properties of the observed structure at $\sqrt{s} = 4.416$ GeV. In the fit, the observed structure is assumed to be a neutral charmoniumlike state with spin-parity 1^+, modeled with an S-wave Breit-Wigner function in two dimensions,

$$\frac{p_1 \cdot q_1/c^2}{(x - M_R^2)^2 + M_R^2 \cdot \Gamma^2/c^4} + \frac{p_2 \cdot q_2/c^2}{(y - M_R^2)^2 + M_R^2 \cdot \Gamma^2/c^4}, \quad (2)$$

taking into account the mass resolution and detection efficiency, where $p_{1/2}$ ($q_{1/2}$) is the momentum of the charmoniumlike state [$\psi(3686)$] in the rest frame of its mother particle and M_R and Γ are the mass and width of the charmoniumlike state, respectively. The PDF of the process $e^+e^- \to \pi^0\pi^0\psi(3686)$ without an intermediate state is taken from the JPIPI model MC simulation. The background is found to be negligible and is not included in the fit. Since the two π^0 mesons in the final state are experimentally indistinguishable, the fit is performed with two entries per event, and the corresponding statistical significance of the observed structure and the errors of the parameters are calculated by doubling the change of likelihood values.

The fit with a width fixed to that of the charged structure observed in $e^+e^- \to \pi^+\pi^-\psi(3686)$ [3] yields a mass of

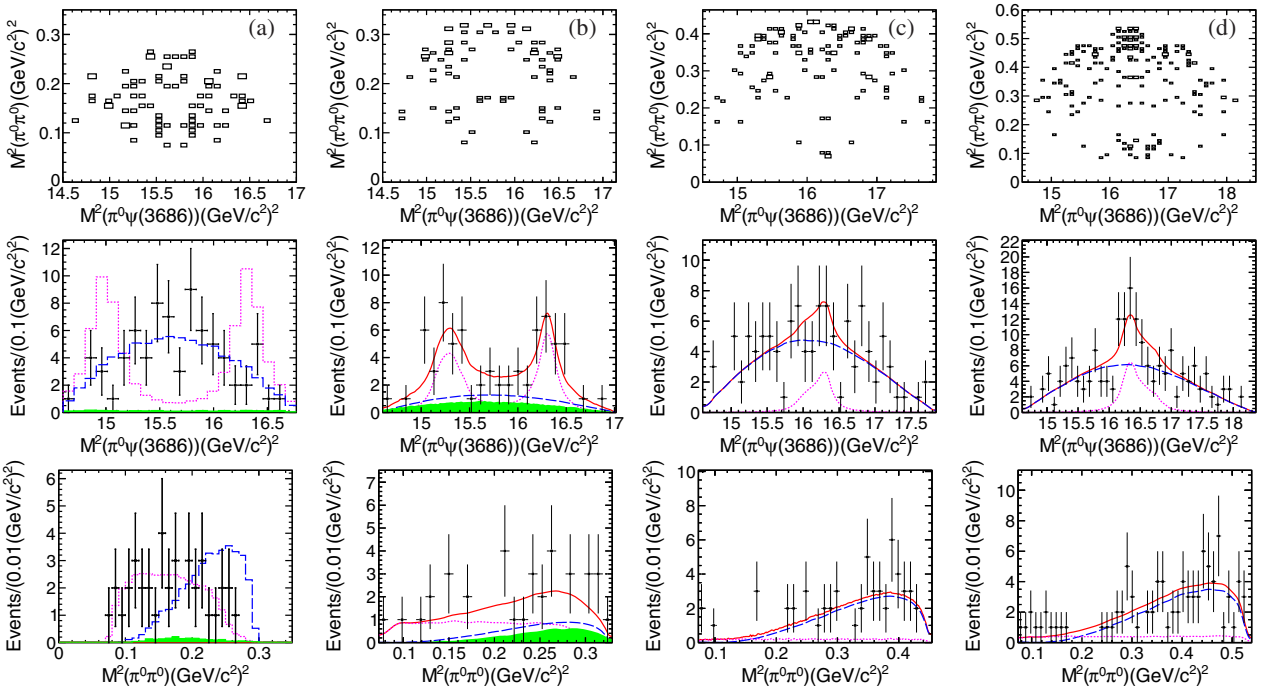

FIG. 3. Dalitz plots of $M^2(\pi^0\pi^0)$ versus $M^2(\pi^0\psi(3686))$ (top row) as well as the distributions of $M^2(\pi^0\psi(3686))$ (middle row) and of $M^2(\pi^0\pi^0)$ (bottom row) for the data samples at $\sqrt{s} = 4.226$ (column a), 4.258 (column b), 4.358 (column c), and 4.416 (column d) GeV. Dots with error bars are data. For plots at $\sqrt{s} = 4.226$ GeV, the short dashed curves (pink) are the distributions for intermediate states, and the blue, long-dashed lines are for the process $e^+e^- \to \pi^0\pi^0\psi(3686)$ simulated with the JPIPI model (both with an arbitrary scale). For plots at 4.258, 4.358, and 4.416 GeV, the solid curves (red) are projections from the fits, the short dashed curves (pink) show the shapes of the intermediate states, and the long dashed curves (blue) show the shapes from the direct process $e^+e^- \to \pi^0\pi^0\psi(3686)$. The green shaded histograms show the background $e^+e^- \to \pi^+\pi^-\psi(3686)$ with the shape fixed to MC simulation.

$M_R = (4038.7 \pm 6.5)$ MeV/c^2 (consistent with that of the charged structure $M = (4032.1 \pm 2.4)$ MeV/c^2 in Ref. [3]) and a statistical significance of 6.0σ (evaluated by comparing the likelihood values with and without the charmoniumlike state included in the fit). The fit projections on $M^2(\pi^0\psi(3686))$ and $M^2(\pi^0\pi^0)$ are shown in Fig. 3. Similar to Ref. [3], the fit curves are found to not match the data perfectly. The C.L. of the fit is 19%, estimated by toy-MC studies. An alternative fit with free width yields a mass of $M_R = (4039.3 \pm 6.0)$ MeV/c^2 and a width of $\Gamma = (31.9 \pm 14.8)$ MeV, which are consistent with those of the charged structure in Ref. [3] within the statistical uncertainties, and a statistical significance of 5.9σ. Another alternative fit with an additional $Z_c(3900)^0$ included is performed, where the parameters of the $Z_c(3900)^0$ are fixed to the weighted average values $M = (3893.6 \pm 3.7)$ MeV/c^2, $\Gamma = (31.1 \pm 7.0)$ MeV in Refs. [21,23]. The statistical significance of the $Z_c(3900)^0$ is less than 1σ. In the fit, the mass and significance of the structure around 4040 MeV/c^2 are similar to the nominal fit results.

Similar fits are carried out to the data samples at $\sqrt{s} = 4.258$ and 4.358 GeV, respectively, where the parameters of the charmoniumlike state are fixed to those obtained in the data sample at $\sqrt{s} = 4.416$ GeV. In the data sample at $\sqrt{s} = 4.258$ GeV, a sizable background from $e^+e^- \to \pi^+\pi^-\psi(3686)$ exists, which is due to the increasing momentum of charged pions, as shown in Fig. 1 with blue dashed curve. It is included in the fit with the shape fixed to the MC simulation and the magnitude extracted from a fit to the $M_{\rm recoil}(\pi^+\pi^-)$ spectrum. The statistical significances of the charmoniumlike structure are 3.6σ and 4.5σ for the data samples at $\sqrt{s} = 4.258$ and 4.358 GeV, respectively. Alternative fits with additional $Z_c(3900)^0$ states included are performed for the data sample at $\sqrt{s} = 4.258$ GeV. Since both $Z_c(3900)^0$ and the structure around 4040 MeV/c^2 are reflected onto each other in the $M(\pi^0\psi(3686))$ spectrum, the statistical significance of $Z_c(3900)^0$ is sensitive to its parameters and is found to be 1.0σ with the parameters above, varied by about 0.6σ when the $Z_c(3900)^0$ parameters are varied within its uncertainties. The fit procedure has been validated with a set of MC samples.

VII. SUMMARY

In summary, based on a data sample of e^+e^- collision data corresponding to 5.2 fb^{-1} at 16 c.m. energy points between 4.009 and 4.600 GeV collected with the BESIII detector, the Born cross sections for $e^+e^- \to \pi^0\pi^0\psi(3686)$ at these energy points have been measured for the first time. They are found to be half of those for $e^+e^- \to \pi^+\pi^-\psi(3686)$ [3] within uncertainties, consistent with the expectation from isospin symmetry. The Dalitz plots of $\pi^0\pi^0\psi(3686)$ are consistent with those in the $e^+e^- \to \pi^+\pi^-\psi(3686)$ [3] at all energy points. Furthermore, a structure is observed in $\pi^0\psi(3686)$ with a mass of (4038.7 ± 6.5) MeV/c^2 at $\sqrt{s} = 4.416$ GeV, which confirms the structure in the charged mode. No obvious $Z_c(3900)^0$ state is observed in the fit. The new observed structure may provide insight into the properties of the charged structure observed in $e^+e^- \to \pi^+\pi^-\psi(3686)$ as well as the charmoniumlike Z_c states observed in analogous decay modes and in charmed meson pairs. However, the fit curve does not match the data perfectly. A future larger statistics sample of data and theoretical input incorporating possible interference effects could lead to a better understanding of the structure.

ACKNOWLEDGMENTS

The BESIII Collaboration thanks the staff of BEPCII and the IHEP computing center and the supercomputing center of USTC for their strong support. This work is supported in part by National Key Basic Research Program of China under Contract No. 2015CB856700; National Natural Science Foundation of China (NSFC) under Contracts No. 11235011, No. 11335008, No. 11425524, No. 11625523, No. 11635010, No. 11375170, No. 11275189, No. 11475164, No. 11475169, No. 11605196, and No. 11605198; the Chinese Academy of Sciences (CAS) Large-Scale Scientific Facility Program; the CAS Center for Excellence in Particle Physics (CCEPP); Joint Large-Scale Scientific Facility Funds of the NSFC and CAS under Contracts No. U1332201, No. U1532257, No. U1532258, and No. U1532102; CAS Key Research Program of Frontier Sciences under Contracts No. QYZDJ-SSW-SLH003 and No. QYZDJ-SSW-SLH040; 100 Talents Program of CAS; National 1000 Talents Program of China; INPAC and Shanghai Key Laboratory for Particle Physics and Cosmology; German Research Foundation DFG under Collaborative Research Center Contracts No. CRC 1044 and No. FOR 2359; Istituto Nazionale di Fisica Nucleare, Italy; Koninklijke Nederlandse Akademie van Wetenschappen (KNAW) under Contract No. 530-4CDP03; Ministry of Development of Turkey under Contract No. DPT2006K-120470; National Natural Science Foundation of China (NSFC) under Contracts No. 11505034 and No. 11575077; National Science and Technology fund; The Swedish Research Council; U.S. Department of Energy under Contracts No. DE-FG02-05ER41374, No. DE-SC-0010118, No. DE-SC-0010504, and No. DE-SC-0012069; University of Groningen (RuG) and the Helmholtzzentrum fuer Schwerionenforschung GmbH (GSI), Darmstadt; and WCU Program of National Research Foundation of Korea under Contract No. R32-2008-000-10155-0

[1] B. Aubert *et al.* (*BABAR* Collaboration), Phys. Rev. Lett. **98**, 212001 (2007); J. P. Lees *et al.* (*BABAR* Collaboration), Phys. Rev. D **89**, 111103 (2014).

[2] X. L. Wang *et al.* (Belle Collaboration), Phys. Rev. Lett. **99**, 142002 (2007); Phys. Rev. D **91**, 112007 (2015).

[3] M. Ablikim *et al.* (BESIII Collaboration), Phys. Rev. D **96**, 032004 (2017).

[4] N. Brambilla *et al.*, Eur. Phys. J. C **71**, 1534 (2011).

[5] B. Aubert *et al.* (*BABAR* Collaboration), Phys. Rev. Lett. **95**, 142001 (2005); J. P. Lees *et al.* (*BABAR* Collaboration), Phys. Rev. D **86**, 051102(R) (2012).

[6] Q. He *et al.* (CLEO Collaboration), Phys. Rev. D **74**, 091104(R) (2006).

[7] C. Z. Yuan *et al.* (Belle Collaboration), Phys. Rev. Lett. **99**, 182004 (2007); Z. Q. Liu *et al.* (Belle Collaboration), Phys. Rev. Lett. **110**, 252002 (2013).

[8] M. Ablikim *et al.* (BESIII Collaboration), Phys. Rev. Lett. **118**, 092001 (2017).

[9] S. L. Zhu, Phys. Lett. B **625**, 212 (2005); E. Kou and O. Pene, Phys. Lett. B **631**, 164 (2005); F. E. Close and P. R. Page, Phys. Lett. B **628**, 215 (2005).

[10] D. Ebert, R. N. Faustov, and V. O. Galkim, Phys. Lett. B **634**, 214 (2006); L. Maiani, V. Riquer, F. Piccinini, and A. D. Polosa, Phys. Rev. D **72**, 031502(R) (2005); T. W. Chiu and T. H. Hsieh (TWQCD Collaboration), Phys. Rev. D **73**, 094510 (2006).

[11] X. Liu, X. Q. Zeng, and X. Q. Li, Phys. Rev. D **72**, 054023(R) (2005); C. F. Qiao, Phys. Lett. B **639**, 263 (2006); C. Z. Yuan, P. Wang, and X. H. Mo, Phys. Lett. B **634**, 399 (2006).

[12] M. Ablikim *et al.* (BESIII Collaboration), Phys. Rev. Lett. **110**, 252001 (2013).

[13] T. Xiao, S. Dobbs, A. Tomaradze, and K. K. Seth, Phys. Lett. B **727**, 366 (2013).

[14] M. Ablikim *et al.* (BESIII Collaboration), Phys. Rev. Lett. **111**, 242001 (2013).

[15] M. Ablikim *et al.* (BESIII Collaboration), Phys. Rev. Lett. **112**, 022001 (2014).

[16] M. Ablikim *et al.* (BESIII Collaboration), Phys. Rev. D **92**, 092006 (2015).

[17] M. Ablikim *et al.* (BESIII Collaboration), Phys. Rev. Lett. **112**, 132001 (2014).

[18] A. Bondar *et al.* (Belle Collaboration), Phys. Rev. Lett. **108**, 122001 (2012).

[19] H. X. Chen, W. Chen, X. Liu, and S.-L. Zhu, Phys. Rep. **639**, 1 (2016).

[20] M. Ablikim *et al.* (BESIII Collaboration), Phys. Rev. Lett. **113**, 212002 (2014).

[21] M. Ablikim *et al.* (BESIII Collaboration), Phys. Rev. Lett. **115**, 222002 (2015).

[22] M. Ablikim *et al.* (BESIII Collaboration), Phys. Rev. Lett. **115**, 182002 (2015).

[23] M. Ablikim *et al.* (BESIII Collaboration), Phys. Rev. Lett. **112**, 132001 (2014).

[24] M. Ablikim *et al.* (BESIII Collaboration), Chin. Phys. C **39**, 093001 (2015).

[25] M. Ablikim *et al.* (BESIII Collaboration), Chin. Phys. C **40**, 063001 (2016).

[26] M. Ablikim *et al.* (BESIII Collaboration), Nucl. Instrum. Methods Phys. Res., Sect. A **614**, 345 (2010).

[27] S. Agostinelli *et al.* (GEANT4 Collaboration), Nucl. Instrum. Methods Phys. Res., Sect. A **506**, 250 (2003).

[28] Z. Y. Deng *et al.*, High Energy Phys. Nucl. Phys. **30**, 371 (2006).

[29] S. Jadach, B. F. L. Ward, and Z. Was, Comput. Phys. Commun. **130**, 260 (2000); Phys. Rev. D **63**, 113009 (2001); A. Fotopoulos and M. Tsulaia, Int. J. Mod. Phys. A **24**, S1 (2009).

[30] T. Mannel and R. Urech, Z. Phys. C **73**, 541 (1997).

[31] R. G. Ping, Chin. Phys. C **32**, 599 (2008); D. J. Lange, Nucl. Instrum. Methods Phys. Res., Sect. A **462**, 152 (2001).

[32] C. Patrignani *et al.* (Particle Data Group), Chin. Phys. C **40**, 100001 (2016).

[33] E. A. Kuraevand and V. S. Fadin, Yad. Fiz. **41**, 733 (1985) [Sov. J. Nucl. Phys. **41**, 466 (1985)].

[34] S. Actis *et al.* Eur. Phys. J. C **66**, 585 (2010).

[35] W. A. Rolke, A. M. Lopez, and J. Conrad, Nucl. Instrum. Methods Phys. Res., Sect. A **551**, 493 (2005).

[36] M. Ablikim *et al.* (BESIII Collaboration), Phys. Rev. Lett. **112**, 022001 (2014); Phys. Rev. D **83**, 112005 (2011).

[37] M. Ablikim *et al.* (BESIII Collaboration), Phys. Rev. D **81**, 052005 (2010).

[38] M. Ablikim *et al.* (BESIII Collaboration), Phys. Rev. D **87**, 012002 (2013).